Desalination and Water Treatment
www.deswater.com

doi: 10.1080/19443994.2015.1093324

57 (2016) 18879–18887
August

Taylor & Francis
Taylor & Francis Group

Adsorption of dispersed red from aqueous solution onto calcined layered double hydroxides: equilibrium, kinetics studies

Yulin Wang, Jianguang Li, Liang Lv*, Guoyun Xv, Yuechao Wu, Jianjun Chen, Wei Hu*

College of Chemical & Materials Engineering, Quzhou University, 78 Jiu Hua Bei Da Dao, Quzhou City, Zhejiang Province 324000, China, Tel. +86 570 8026667; Fax: +86 570 8026552; emails: Lianglv_qzxy@126.com (L. Lv), hw@qzu.zj.cn (W. Hu)

Received 14 January 2014; Accepted 7 September 2015

ABSTRACT

Calcined layered double hydroxides (CLDHs) were used as an adsorbent to remove an azo dye—dispersed red (DR), from aqueous solution by the batch adsorption technique. Various conditions were evaluated, including CLDH structures, adsorbent dosage, initial dye concentration, and temperature. It was found that the layered double hydroxides with a Mg/Al ratio of 3 calcined at 500℃ had the highest capacity for adsorption of DR. The adsorption capacity of CLDH decreased with increasing adsorbent dose, but increased with increasing initial DR concentration. The data of sorption isotherms fitted well into the Langmuir equation. Thermodynamic parameters such as ΔG°, ΔH°, and ΔS° were calculated. The negative values of ΔG° indicate the spontaneous nature of adsorption of DR. The positive value of ΔH° confirms the endothermic nature of the removal process. The positive value of ΔS° suggests the increased randomness at the solid/solution interface for the adsorption of DR onto CLDHs. The results of two kinetic models which fitted the experimental data show that the pseudo-first-order kinetic model gave a better description for the adsorption process. The rate constants and activation energy of adsorption were also calculated. The calculated value of E_a was 14.50 kJ/mol, which indicates that the adsorption process was controlled by diffusion.

Keywords: Layered double hydroxides; Calcined; Removal; Dispersed red; Dye

1. Introduction

Mankind has used dyes for thousands of years [1]. A few decades earlier, the dyes selection, application, and use were not given a major consideration with respect to their environmental impact. Even the chemical composition of half of the dyes used in the industry was estimated to be unknown. With the growing concern on health, mainly on esthetic grounds, it was more from the 80s that people started paying much attention to the dye wastes too [2]. Most of the dyes released during textiles, clothing, printing, and dyeing processes are considered as hazardous and toxic to some organisms and may cause direct destruction of aquatic creatures [3]. In the last few years, however, more information on the environmental consequences of dyestuff usage has become available and the dye manufacturers, users, and governments themselves are taking substantial measures to treat the dye containing wastewaters.

Dispersed red (DR) is a kind of azo dye. Its chemical structural formula is as follows:

---

*Corresponding authors.

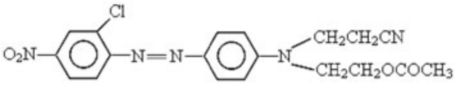

Several methods have been used to treat the dye containing wastewaters, such as sedimentation [4], filtration technology [5], chemical treatment [6,7], oxidation [8–11], electrochemical methodology [12–15], ion exchange [16,17], biological treatment [18–21], and photocatalyst degradation [22]. In addition to the already mentioned methods, the adsorption process which besides being widely used for dye removal also has a wide applicability in wastewater treatment [23–27]. In recent years, many studies have focused on seeking cheap, locally available, and effective adsorbents, such as waste biopolymers [28,29], clays, and clay minerals [30–34]. Among these materials, layered double hydroxides (LDHs) have higher adsorption capacities and are recyclable [35].

LDHs, a class of synthetic clays with high anion-exchange capacities, are effective adsorbents to remove lots of anionic pollutants. The chemical composition of LDHs can be described by the formula $[M^{2+}{}_{1-x}M^{3+}{}_{x}(OH)_2]^{x+}(A^{n-})_{x/n}\cdot mH_2O$ where M^{2+} and M^{3+} are metal cations, for example, Mg^{2+} and Al^{3+}, that occupy octahedral sites in the hydroxide layers, A^{n-} is an exchangeable anion, and x is the ratio $M^{3+}/(M^{2+}+M^{3+})$ [35,36]. The decomposition of MgAl-CO_3 LDHs when heated around 500°C leads to mixed metal oxides, which are characterized by high specific surface areas and homogeneous dispersion of metal cations. The mixed metal oxides can take up anions from the aqueous solution, with concomitant reconstruction of the original layered structure. Therefore, the calcined layered double hydroxides (CLDHs) can be used as potential adsorbents to remove toxic anions from contaminated water [35–40].

The purpose of this work was to investigate the removal of DR from wastewater by CLDHs, by taking into account the effects of CLDH structures, adsorbent dosage, initial dye concentration, and temperature. The results reported here show that these factors affect the adsorption of DR and are significant toward a better understanding of the potential application of CLDHs for decolorization of the dye wastewater.

2. Materials and methods

2.1. Materials

$Mg(NO_3)_2\cdot 6H_2O$, $Al(NO_3)_3\cdot 9H_2O$, NaOH, Na_2CO_3, and NaCl were analytical reagent (A.R.) grade, used as received. DR was provided by Hangzhou Caltex Chemical Co., Ltd. All the water used was deionized. MgAl-CO_3 LDHs were obtained using a conventional co-precipitation method [41,42]. The method involves very rapid mixing to complete the nucleation process, followed by a separate aging process. CLDHs were obtained by calcining LDHs in a muffle furnace at the designation temperature (500°C) for 3 h.

2.2. Characterization

X-ray diffraction pattern of the samples, including MgAl-CO_3 LDHs, CLDHs, and CLDHs after adsorption of DR, was obtained using a Shimadzu XRD-6000 diffractometer with Cu Kα radiation (40 kV and 30 mA) at a scanning rate of $5^\circ\,min^{-1}$. Elemental analysis was performed by inductively coupled plasma (ICP) emission spectroscopy with a Shimadzu ICPS-7500 ICP instrument using solutions prepared by dissolving the samples in dilute HNO_3.

2.3. Sorption experiments

All sorption studies were carried out in a series of 100 mL conical flasks by subjecting a given dose of CLDH to a period of reciprocating type shaking together with the DR synthetic wastewater (50 ml) at 30°C. The adsorbent was separated by filtration, and the filtrate was analyzed for DR concentration using spectrophotometric method. Blanks containing no DR were used for each series of experiments. The DR concentration, the percentage removal of DR, and the adsorption capacity of CLDH for DR were calculated from the concentrations in solution before and after adsorption, respectively.

Sorption isotherm studies were conducted in a series of 100 mL flask by mixing 50 mL of DR solution (0.05–1 mmol/L) with 0.05 g CLDH. The mixture was shaken at the designation temperature for 24 h to allow the adsorption of DR until the equilibrium was reached. The pH of the solution was not adjusted. After shaking for 24 h, the mixture was then filtered. The DR concentration was measured using spectrophotometric method. The adsorption capacity was calculated by the following equation:

$$q_e = \frac{(C_0 - C_e)V}{m} \tag{1}$$

where q_e is the adsorption capacity at the equilibrium in mmol/g, C_0 and C_e are initial and equilibrium concentrations of DR in mmol/L, V is the volume of solution in liters, and m is the mass of CLDH in grams.

Kinetic studies were conducted in a series of 100 mL flask by mixing 50 mL of DR solution (1 mmol/L) with 0.1 g CLDH. The mixture was shaken at a certain temperature (e.g. 30℃), in N_2 atmosphere. The pH of the solution was not adjusted. After shaking for the designated time, the mixture was then filtered. DR concentration was measured using spectrophotometric method, and the solid remaining at the end of the experiment was characterized by X-ray diffraction. The DR uptake by the CLDH was calculated from the following equation:

$$q_t = \frac{(C_0 - C_t)V}{m} \tag{2}$$

where q_t is the adsorption capacity of CLDH at time t in mmol/g, V is the volume of solution in liters, C_0 and C_t are the initial concentration of DR and that at time t in mmol/L, and m is the mass of CLDH in grams.

3. Results and discussion

3.1. Effect of Mg/Al molar ratio of LDHs layers

The effect of varying Mg/Al molar ratio of LDHs on the adsorption of DR was investigated. It can be seen from Table 1 that the retention of DR by the CLDH with Mg/Al molar ratio of 3 is the best of all, for which the adsorption capacity 0.33 mmol/g in the initial DR concentration is 0.5 mmol/L. The Mg/Al molar ratio has only a slight influence on the adsorption capacity. The percentage of removal is 82.1%, slightly higher than the Mg/Al ratios of 2 (78.6%) and 4 (80.8%).

3.2. Effect of dosage of CLDHs

The effect of the dosage of CLDHs on the adsorption of DR with initial concentration of 0.2 mmol/L was studied and the results were shown in Fig. 1. It can be seen that the dosage of CLDH significantly influenced the removal of DR. The percentage removal of DR was 43.1% for 0.5 g/L of CLDH, while it was greatly increased to 79.6% for 1.0 g/L of adsorbent. However, there was only a slight change in the extent of adsorption of DR when the dosage of adsorbent was over 1.0 g/L. For example, the percentage removal was 82.1% for 2.0 g/L of adsorbent.

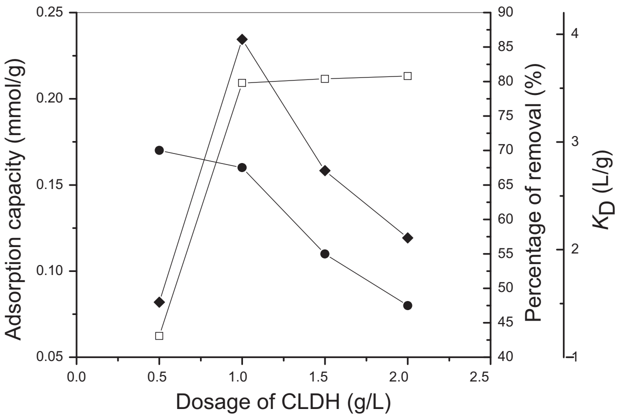

Fig. 1. Effect of adsorbent dose on the adsorption of DR: (●) adsorption capacity vs. dosage of CLDH, (□) percentage of removal vs dosage of CLDH, and (♦) distribution coefficient K_D vs. dosage of CLDH (V = 50 ml, [DR] = 0.2 mmol/L, T = 25℃).

Furthermore, the higher adsorbent dose results in a lower adsorption capacity of CLDH at a fixed DR concentration (0.2 mmol/L), as shown in Fig. 1, consistent with the argument that the surface sites of the adsorbent are heterogeneous. According to the surface site heterogeneity model, the surface is composed of sites with a spectrum of binding energies. At low adsorbent dose, all types of sites are entirely exposed and the adsorption on the surface is saturated fast, showing a high adsorption capacity. But at a high adsorbent dose, the availability of higher energy sites

Table 1
Effect of Mg/Al molar ratio on the adsorption of DR

$[DR]_0$ (mmol/L)	Mg/Al ratio	$[DR]_t$ (mmol/L)	Percentage of removal (%)	Adsorption capacity (mmol/g)
0.1	2	0.0421	57.9	0.06
0.1	3	0.0337	66.3	0.07
0.1	4	0.0340	66.0	0.07
0.2	2	0.0427	78.6	0.16
0.2	3	0.0357	82.1	0.16
0.2	4	0.0383	80.8	0.16
0.5	2	0.2124	57.5	0.29
0.5	3	0.1714	65.7	0.33
0.5	4	0.2019	59.6	0.30

decreases with a larger fraction of lower energy sites occupied, resulting in a low adsorption capacity.

The distribution coefficient K_D (L/g), describing the binding ability of adsorbent surface for an element, was calculated as Eq. (3):

$$K_D = C_s/C_w \tag{3}$$

where C_s is the concentration of DR on solids (mmol/g) and C_w is the concentration of DR in water (mmol/L).

It can be seen from Fig. 1 that the distribution coefficient (K_D) increases with increasing dosage of CLDH in the range of 0.5–1.0 g/L and decreases with increasing dosage of CLDH in the range of 1.0–2.0 g/L, which also implies that the surface of CLDH is heterogeneous. If the surface is homogeneous, the K_D values should not change with adsorbent dosage.

3.3. Effect of initial DR concentration

The effect of the initial DR concentration on the adsorption of DR onto the CLDH was studied and shown in Fig. 2. It can be seen from Fig. 2(A) that the percentage of removal increases with the decrease in the initial DR concentration. When the initial concentration of DR is 0.2 mmol/L, the percentage of removal is higher than 80%. At the same time, it is obvious in Fig. 2(B) that the adsorption capacity of CLDH increases with the increase in the initial DR concentration. And the adsorption capacity of CLDH decreased with the increase in the dosage of CLDH. Because the adsorption capacity (q_e) was inversely proportional to the mass of CLDH.

3.4. Equilibrium isotherm

Fig. 3 is the equilibrium isotherm of adsorption of DR onto CLDH at different temperatures, which indicates that the adsorption capacity increases upon increasing equilibrium concentration of DR and increasing temperature. The temperature dependence of adsorption process is associated with several thermodynamic parameters.

Two general-purpose equilibrium models were used in an attempt to fit the experimental data: (i) the Langmuir model (Eq. (4)) and (ii) the Freundlich model (Eq. (5)), respectively, and it was found that the Langmuir model gave a satisfactory fit to the experimental data, as shown in Table 2.

$$q_e = \frac{q_m K_L C_e}{1 + K_L C_e} \tag{4}$$

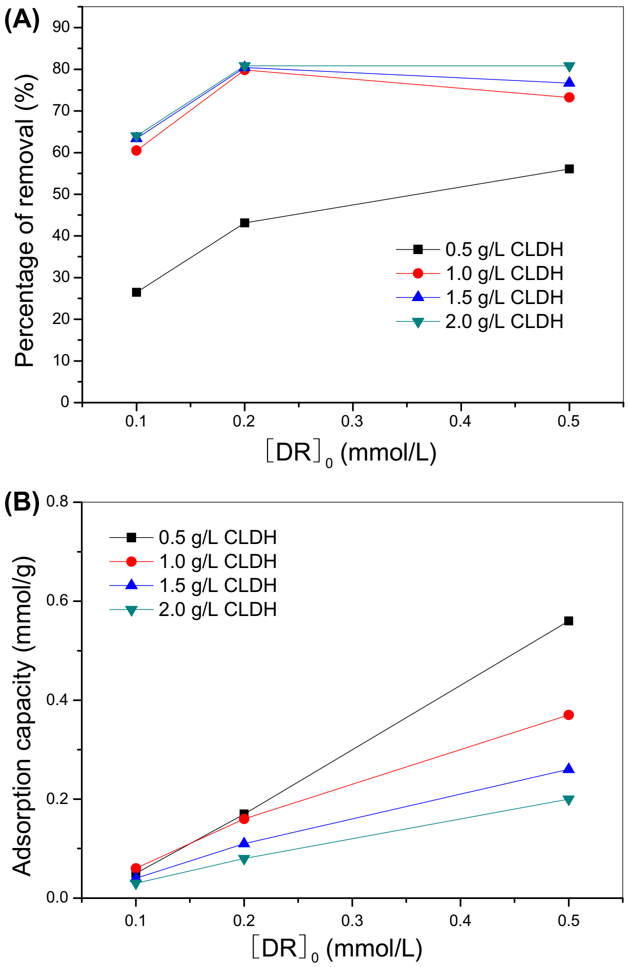

Fig. 2. Effect of initial concentration on te adsorption of DR (V = 50 ml, T = 25℃).

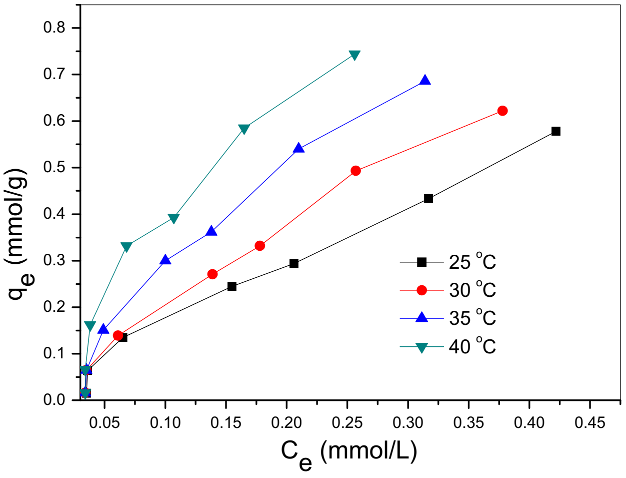

Fig. 3. Equilibrium isotherms for adsorption of DR onto CLDH.

Table 2
Freundlich, Langmuir constants, and thermodynamic parameters associated with adsorption of DR onto CLDH

	Freundlich			Langmuir				Thermodynamic parameters		
Temp. (℃)	K_F	n	R^2	q_m (mmol/g)	K_L (L/mol)	ln K_L	R^2	ΔG° (kJ/mol)	ΔH° (kJ/mol)	ΔS° (J/mol/K)
25	1.253	0.905	0.987	3.47	465.81	6.144	0.986	−15.23	70.67	287.91
30	1.552	0.900	0.981	2.93	734.14	6.599	0.986	−16.63		
35	2.033	0.900	0.966	2.77	1,084.85	6.989	0.939	−17.91		
40	2.582	0.873	0.929	2.68	1,866.05	7.532	0.973	−19.61		

$$q_e = K_F C_e^n \tag{5}$$

where K_L is the Langmuir constant related to the loading and energy of adsorption in L/mol, K_F and n are the Freundlich temperature-dependent constants, q_m is the maximum adsorption capacity in mmol/g, q_e is the adsorption capacity at equilibrium in mmol/g, and C_e is the equilibrium concentration of DR in the solution in mmol/L, respectively.

Thermodynamic parameters such as Gibbs free energy (ΔG°), standard enthalpy change (ΔH°), and standard entropy change (ΔS°) for the process were calculated using the equations:

$$\Delta G^\circ = -RT \ln K_L \tag{6}$$

$$\ln K_L = \Delta S^\circ / R - \Delta H^\circ / (RT) \tag{7}$$

where R is universal gas constant, T is temperature (K), and K_L is Langmuir constant.

The values of ΔG°, ΔH°, and ΔS° are also listed in Table 2. The negative ΔG° value indicates the spontaneity of the DR removal process. ΔH° and ΔS° were calculated from a Van't Hoff plot (Fig. 4, correlation coefficient $R^2 = 0.997$) using the slope, and intercept by regression method, respectively. The positive value of ΔH° confirms the endothermic nature of adsorption DR onto CLDH. The positive value of ΔS° suggests the increased randomness at the solid/solution interface for the adsorption process.

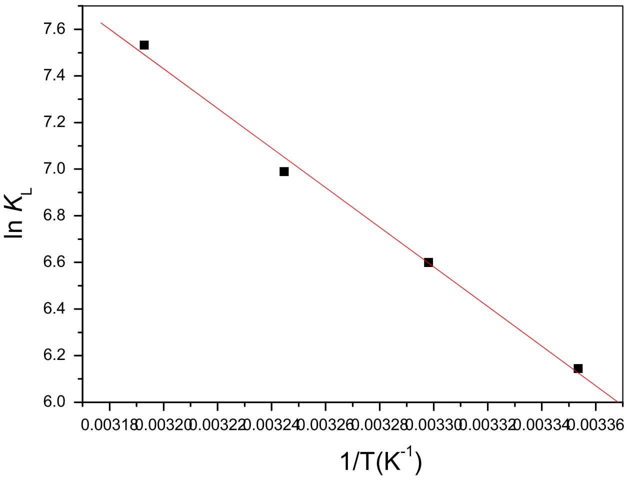

Fig. 4. Van't Hoff plot for adsorption of DR onto CLDH.

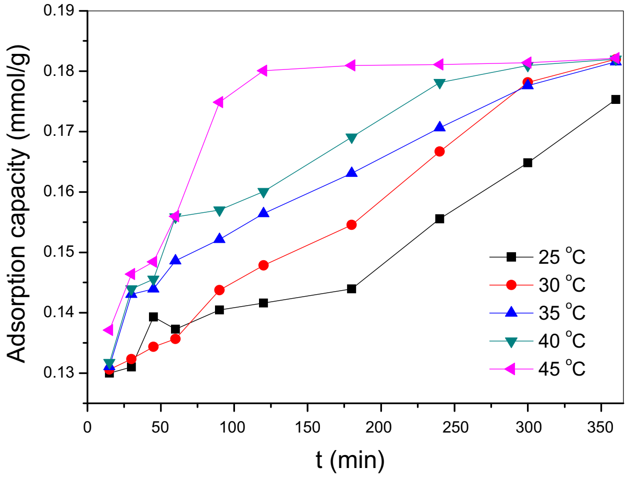

Fig. 5. Kinetics of the adsorption of DR onto CLDH (V = 50 ml, $[DR]_0$ = 1 mmol/L, [CLDH] = 2.0 g/L).

3.5 Kinetic studies

Kinetic studies of the removal of DR by LDHs were concerned with obtaining essential information to enable the adsorbent to be used in practical treatment systems. Fig. 5 shows the experimental data obtained under different isothermal conditions. The rate of adsorption increases significantly with temperature and the time taken to reach equilibrium decreases with increasing temperature.

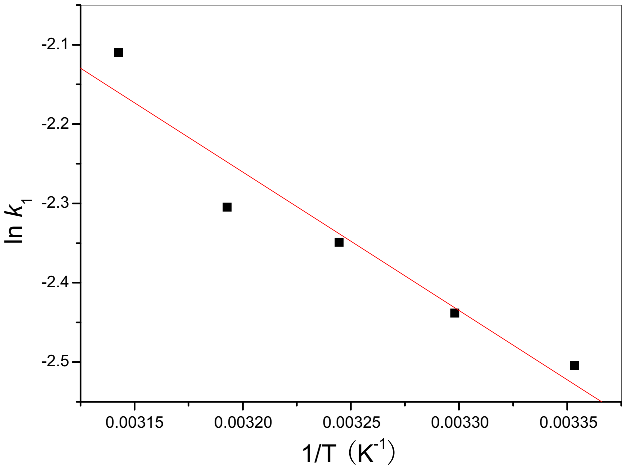

Fig. 6. Arrhenius plot for adsorption of DR onto CLDH.

Table 3 presents the results of fitting experimental data to first-order (Eq. (8)) and pseudo-second-order (Eq. (9)) models, respectively.

$$\frac{dq_t}{dt} = k_1(q_e - q_t) \tag{8}$$

$$\frac{dq_t}{dt} = k_2(q_e - q_t)^2 \tag{9}$$

where q_t is the adsorption capacity at time t in mmol/g, and q_e is the adsorption capacity at equilibrium in mmol/g, respectively.

It can be seen from Table 3 that the correlation coefficient (R^2) varies in the order: first-order model > pseudo-second-order under all experimental conditions, which indicates that the first-order model is the most satisfactory in describing the adsorption kinetics of DR onto CLDH. The experimental q_e values agree well with the calculated ones obtained from the first-order kinetics model.

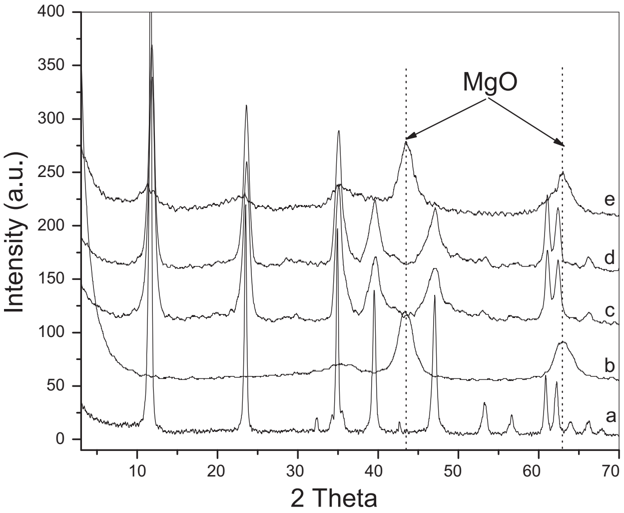

Fig. 7. XRD patterns of (a) MgAl-CO_3 LDH precursor, (b) calcined LDH (CLDH), (c) CLDH after adsorption DR, (d) material regenerated by treating the resulting adsorbent with Na_2CO_3 aqueous solution, and (e) material regenerated by direct calcination of the resulting adsorbent.

An Arrhenius plot of the adsorption rate against the reciprocal temperature was performed using the kinetic data of Table 3, giving a reasonably straight line (Fig. 6, $R^2 = 0.996$). The gradient of this plot is $-(E_a/R)$, according to the well-known Arrhenius expression given in Eq. (10), and the activation energy can thus be calculated:

$$k_1 = A\,e^{-(E_a/RT)} \tag{10}$$

For diffusion-controlled processes, the activation energy of adsorption is lower than 20 kJ/mol. The calculated E_a value in our case, 14.5 kJ/mol, indicates that the process of dye removal is controlled by DR diffusion onto CLDH.

Table 3
Experimental conditions, kinetic parameters, and regression coefficients (R^2) for the two kinetic models

					Pseudo-first-order			Pseudo-second-order		
Run no.	$[DR]_0$ (mmol/L)	[CLDH] (g/L)	Temp. (℃)	$q_{e\ exp}$ (mmol/L)	$q_{e\ cal}$ (mmol/g)	$k_1 \times 10^{-2}$ (min^{-1})	R^2	$q_{e\ cal}$ (mmol/g)	k_2 (g/mmol min)	R^2
1	1	2.0	25	0.175	0.149	12.12	0.923	0.157	1.378	0.501
2	1	2.0	30	0.181	0.155	9.98	0.993	0.167	0.955	0.568
3	1	2.0	35	0.181	0.162	9.55	0.979	0.172	0.868	0.757
4	1	2.0	40	0.180	0.166	8.73	0.972	0.177	0.853	0.826
5	1	2.0	45	0.182	0.174	8.17	0.650	0.184	0.803	0.856

Table 4
Relationship between the percentage of removal, adsorption capacity, and number of times recycled ($T = 30$℃, [DR] = 50 mg/L, [CLDH] = 2.0 g/L)

Cycle number	Percentage of removal (%)	Adsorption capacity (mmol/g)
1	98.1	44.14
2	97.7	43.96
3	98.0	44.10
4	97.3	43.78
5	96.9	43.60

3.6. Regeneration studies

In order to recycle the adsorbent, it is necessary to regenerate the resulting adsorbent. There are two methods to regenerate the adsorbent. The first one was carried out using Na_2CO_3 aqueous solution (0.1 M). The mixture was stirred for 6 h, and the resulting solid was then filtered, washed thoroughly with deionized water, and calcined in a muffle furnace at 500℃ for 3 h. The other regeneration method was direct calcination of the resulting adsorbent.

Fig. 7(a) that the XRD pattern of the MgAl-CO_3 LDHs precursor shows sharp and symmetric peaks at lower 2θ values, which are characteristic of hydrotalcite-like compounds, and the material consists of a single crystalline phase. After the LDHs precursor was calcined at 500℃, the layered structure is lost (Fig. 7(b)), leading to the formation of a mixed magnesium aluminum oxide. Reconstruction of the structure (Fig. 7(c)) has been observed to take place after adsorption DR, giving a material having a basal spacing (d 0 0 3) of 0.756 nm, the same as that (0.755 nm) of the MgAl-CO_3 LDH precursor. This indicates that the dye molecules did not enter the interlayer of LDHs. However, material regenerated by direct calcination of the resulting adsorbent (Fig. 7(e)) was the formation of a mixed magnesium aluminum oxide, the same as CLDH.

Successive adsorption measurements (Table 4) show that the regenerated CLDH has almost the same capability to remove DR as a fresh one. So it can be concluded that the wastewater treatment is a reversible process, thereby facilitating the recycling of the material for further use.

4. Conclusions

These studies have significant implications for efficient remediation of DR from aqueous solution by CLDHs, and the process is reversible. The adsorption capacity of CLDHs increases with the increase in the initial DR concentration, but decreases with increasing temperature. Thermodynamic parameters were calculated. The negative ΔG° value indicates the spontaneity of the DR removal process. The positive value of ΔH° confirms the endothermic nature of DR removal. The positive value of ΔS° suggests the increased randomness at the solid/solution interface for the adsorption of DR onto CLDHs. Adsorption of DR by CLDH follows the pseudo-first-order model, which describes the DR diffusion onto CLDH process.

Acknowledgments

This work was partially supported by the National Natural Science Foundation (21271116, 21476127), the Public Technology Research Program of Zhejiang Province (2013C31108, 2013C33018, 2015C33231), the State Key Laboratory of Chemical Resource Engineering, the Natural Science Foundation of Zhejiang Province, and the Science Technology Department of Quzhou City, and Special Funds of Faculty Building in Quzhou University.

References

[1] R.M. Christie, Environmental Aspects of Textile Dyeing, CRC Press, Woodhead; Boca Raton, FL, 2007.
[2] V.K. Gupta, Suhas, Application of low-cost adsorbents for dye removal—A review, J. Environ. Manage. 90 (2009) 2313–2342.
[3] H.-Y. Zhu, R. Jiang, L. Xiao, Adsorption of an anionic azo dye by chitosan/kaolin/γ-Fe_2O_3 composites, Appl. Clay Sci. 48 (2010) 522–526.
[4] N.P. Cheremisinoff, Handbook of Water and Wastewater Treatment Technologies, Butterworth-Heinemann, Boston, MA, 2002.
[5] S.A. Avlonitis, I. Poulios, D. Sotiriou, M. Pappas, K. Moutesidis, Simulated cotton dye effluents treatment and reuse by nanofiltration, Desalination 221 (2008) 259–267.
[6] B.Y. Shi, G.H. Li, D.S. Wang, C.H. Feng, H.X. Tang, Removal of direct dyes by coagulation: The performance of preformed polymeric aluminum species, J. Hazard. Mater. 143 (2007) 567–574.

[7] Y. Zhou, Z. Liang, Y. Wang, Decolorization and COD removal of secondary yeast wastewater effluents by coagulation using aluminum sulfate, Desalination 225 (2008) 301–311.

[8] R. Hage, A. Lienke, Applications of transition-metal catalysts to textile and wood-pulp bleaching, Angew. Chem. Int. Ed. 45 (2006) 206–222.

[9] J. Wu, H. Doan, S. Upreti, Decolorization of aqueous textile reactive dye by ozone, Chem. Eng. J. 142 (2008) 156–160.

[10] M. Eskandarian, F. Mahdizadeh, L. Ghalamchi, S. Naghavi, Bio-Fenton process for Acid Blue 113 textile azo dye decolorization: Characteristics and neural network modeling, Desalin. Water Treat. 52 (2014) 4990–4998.

[11] A. Zuorro, R. Lavecchia, Evaluation of UV/H_2O_2 advanced oxidation process (AOP) for the degradation of diazo dye Reactive Green 19 in aqueous solution, Desalin. Water Treat. 52 (2014) 1571–1577.

[12] V.K. Gupta, R. Jain, S. Varshney, Electrochemical removal of the hazardous dye Reactofix Red 3 BFN from industrial effluents, J. Colloid Interface Sci. 312 (2007) 292–296.

[13] D. Dogan, H. Turkdemir, Electrochemical oxidation of textile dye indigo, J. Chem. Technol. Biotechnol. 80 (2005) 916–923.

[14] A.M. Faouzi, B. Nasr, G. Abdellatif, Electrochemical degradation of anthraquinone dye Alizarin Red S by anodic oxidation on boron-doped diamond, Dyes Pigm. 73 (2007) 86–89.

[15] F.H. Oliveira, M.E. Osugi, F.M.M. Paschoal, D. Profeti, P. Olivi, M.V.B. Zanoni, Electrochemical oxidation of an acid dye by active chlorine generated using Ti/$Sn_{(1-x)}Ir_xO_2$ electrodes, J. Appl. Electrochem. 37 (2007) 583–592.

[16] C.-H. Liu, J.-S. Wu, H.-C. Chiu, S.-Y. Suen, K.H. Chu, Removal of anionic reactive dyes from water using anion exchange membranes as adsorbers, Water Res. 41 (2007) 1491–1500.

[17] S. Raghu, C. Ahmed Basha, Chemical or electrochemical techniques, followed by ion exchange, for recycle of textile dye wastewater, J. Hazard. Mater. 149 (2007) 324–330.

[18] B.E. Barragan, C. Costa, M. Carmen Marquez, Biodegradation of azo dyes by bacteria inoculated on solid media, Dyes Pigm. 75 (2007) 73–81.

[19] C.T.M.J. Frijters, R.H. Vos, G. Scheffer, R. Mulder, Decolorizing and detoxifying textile wastewater, containing both soluble and insoluble dyes, in a full scale combined anaerobic/aerobic system, Water Res. 40 (2006) 1249–1257.

[20] F.M. Zhang, J.S. Knapp, K.N. Tapley, Decolourisation of cotton bleaching effluent in a continuous fluidized-bed bioreactor using wood rotting fungus, Biotechnol. Lett. 20 (1998) 717–723.

[21] D. Haddaji, L. Bousselmi, O. Saadani, I. Nouairi, Z. Ghrabi-Gammar, Enzymatic degradation of azo dyes using three macrophyte species: *Arundo donax*, *Typha latifolia* and *Phragmites australis*, Desalin. Water Treat. 53 (2015) 1126–1135.

[22] S. Xia, F. Liu, Z. Ni, W. Shi, J. Xue, P. Qian, Ti-based layered double hydroxides: Efficient photocatalysts for azo dyes degradation under visible light, Appl. Catal. B: Environ. 144 (2014) 570–579.

[23] R.C. Bansal, M. Goyal, Activated Carbon Adsorption, Taylor & Francis, Boca Raton, FL, 2005.

[24] T.G. Danis, T.A. Albanis, D.E. Petrakis, P.J. Pomonis, Removal of chlorinated phenols from aqueous solutions by adsorption on alumina pillared clays and mesoporous alumina aluminum phosphates, Water Res. 32 (1998) 295–302.

[25] K. Imamura, E. Ikeda, T. Nagayasu, T. Sakiyama, K. Nakanishi, Adsorption behavior of methylene blue and its congeners on a stainless steel surface, J. Colloid Interface Sci. 245 (2002) 50–57.

[26] F. Quignon, F. Thomas, C. Gantzer, A. Huyard, L. Schwartzbrod, Virus adsorption in a complex system: An experimentally designed study, Water Res. 32 (1998) 1222–1230.

[27] P. Liu, P. Liu, K. Zhao, L. Li, Photostability enhancement of azoic dyes adsorbed and intercalated into Mg–Al-layered double hydroxide, Opt. Laser Technol. 74 (2015) 23–28.

[28] G. Crini, P.M. Badot, Application of chitosan, a natural aminopolysaccharide, for dye removal from aqueous solutions by adsorption processes using batch studies: A review of recent literature, Prog. Polym. Sci. 33 (2008) 399–447.

[29] W.H. Cheung, Y.S. Szeto, G. McKay, Enhancing the adsorption capacities of acid dyes by chitosan nano particles, Bioresour. Technol. 100 (2009) 1143–1148.

[30] D.S. Tong, M. Liu, L. Li, C.X. Lin, W.H. Yu, Z.P. Xu, C.H. Zhou, Transformation of alunite residuals into layered double hydroxides and oxides for adsorption of acid red G dye, Appl. Clay Sci. 70 (2012) 1–7.

[31] H. Gecol, P. Miakatsindila, E. Ergican, S.R. Hiibel, Biopolymer coated clay particles for the adsorption of tungsten from water, Desalination 197 (2006) 165–178.

[32] A.B. Karim, B. Mounir, M. Hachkar, M. Bakasse, A. Yaacoubi, Removal of Basic Red 46 dye from aqueous solution by adsorption onto Moroccan clay, J. Hazard. Mater. 168 (2009) 304–309.

[33] Q. Tang, X.W. Tang, Z.Z. Li, Y.M. Chen, N.Y. Kou, Z.F. Sun, Adsorption and desorption behaviour of Pb (II) on a natural kaolin: Equilibrium, kinetic and thermodynamic studies, J. Chem. Technol. Biotechnol. 84 (2009) 1371–1380.

[34] V. Vimonses, S. Lei, B. Jin, C.W.K. Chow, C. Saint, Adsorption of congo red by three Australian kaolins, Appl. Clay Sci. 43 (2009) 465–472.

[35] F. Cavani, F. Trifirò, A. Vaccari, Hydrotalcite-type anionic clays: Preparation, properties and applications, Catal. Today 11 (1991) 173–301.

[36] S. Miyata, Physico-chemical properties of synthetic hydrotalcites in relation to composition, Clays Clay Miner. 28 (1980) 50–56.

[37] L. Ei Gaini, M. Lakraimi, E. Sebbar, A. Meghea, M. Bakasse, Removal of indigo carmine dye from water to Mg–Al–CO_3 calcined layered double hydroxides, J. Hazard. Mater. 161 (2009) 627–632.

[38] D.P. Das, J. Das, K. Parida, Physicochemical characterization and adsorption behavior of calcined Zn/Al hydrotalcite-like compound (HTlc) towards removal of fluoride from aqueous solution, J. Colloid Interface Sci. 261 (2003) 213–220.

[39] N.K. Lazaridis, D.D. Asouhidou, Kinetics of sorptive removal of chromium(VI) from aqueous solutions by calcined Mg–Al–CO_3 hydrotalcite, Water Res. 37 (2003) 2875–2882.

[40] Y. Zhao, W. Hu, J. Chen, L. Lv, Factors influencing the chloride removal of aqueous solution by calcined layered double hydroxides, Desalin. Water Treat. 36 (2011) 50–56.

[41] X. Duan, Q.Z. Jiao, L. Li, New method of synthesis the uniform dispersion and superfine layered double hydroxides, CN 1288076, 2001-03-21.

[42] L.L. Ren, J. He, D.G. Evans, X. Duan, R.Y. Ma, Some factors affecting the immobilization of penicillin G acylase on calcined layered double hydroxides, J. Mol. Catal. B: Enzym. 16 (2001) 65–71.